

Aluminum arsenide cleaved-edge overgrown quantum wires

J. Moser,¹ T. Zibold,¹ S. Roddaro,² D. Schuh,¹ M. Bichler,¹ V. Pellegrini,² G. Abstreiter,¹ and M. Grayson¹¹Walter Schottky Institut, Technische Universität München, D-85748 Garching, Germany²Scuola Normale Superiore, via della Faggiola, I-56126 Pisa, Italy

(Dated: 28 Feb 2005)

We report conductance measurements in quantum wires made of aluminum arsenide, a heavy-mass, multi-valley one-dimensional (1D) system. Zero-bias conductance steps are observed as the electron density in the wire is lowered, with additional steps observable upon applying a finite dc bias. We attribute these steps to depopulation of successive 1D subbands. The quantum conductance is substantially reduced with respect to the anticipated value for a spin- and valley-degenerate 1D system. This reduction is consistent with disorder-induced, intra-wire backscattering which suppresses the transmission of 1D modes. Calculations are presented to demonstrate the role of strain in the 1D states of this cleaved-edge structure.

One-dimensional systems of heavy electrons (effective mass $m^* = m_0$, where m_0 is the free electron mass) are promising candidates for the study of electronic correlations. However owing to an inherent low mobility

and fabrication challenges, few realizations are reported in the literature. Experiments in Si [1, 2] and Si/SiGe [3, 4] quantum point contacts (QPC) have only focused on transport in (100)-plane structures with light isotropic mass $m^* = 0.19m_0$. A conductance step height $G_0 = g_s g_v e^2/h = 4e^2/h$ was found in the ballistic regime [3], accounting for both spin $g_s = 2$ and valley $g_v = 2$ degeneracy, and $G_0 = 2e^2/h$ was observed in those systems in the presence of disorder [3]. Aluminum arsenide (AlAs) is an alternate heavy mass system with degenerate valleys and anisotropic mass. In AlAs the constant energy surfaces are ellipses centered at the X_i points ($i = x, y, z$) at the Brillouin zone edge, characterized by a heavy longitudinal mass $m_H = 1.1m_0$ and light transverse mass $m_L = 0.19m_0$ [5]. The energy minima at these X points are highly sensitive to strain [6].

In this paper we report conductance measurements of a quantum wire fabricated at the edge of an aluminum arsenide (AlAs) 2D-electron gas (2DEG) using cleaved-edge overgrowth (CEO). In absence of interactions a valley degeneracy $g_v = 2$ is predicted in the wire. Two conductance steps are observed at low electron density, with step height $G_0 = 0.44e^2/h$. Applying a finite dc bias across the wire reveals cleaner steps of the same height. We discuss the role of strain, disorder and interactions in relation to the observed 1D conductance.

AlAs wires are fabricated with the same CEO technique employed for ballistic GaAs wires [7]. Our samples contain a modulation-doped AlAs quantum well [8] flanked by two $\text{Al}_x\text{Ga}_{1-x}\text{As}$ dielectric barriers ($x = 0.45$) and grown onto a [001]-oriented GaAs substrate by molecular beam epitaxy (MBE). The 150 Å wide quantum well resides 4000 Å below the surface with density $n = 5.6 \times 10^{11} \text{ cm}^{-2}$ and mobility $\mu = 55,000 \text{ cm}^2/\text{Vs}$ at $T = 340 \text{ mK}$. A 1 μm -wide tantalum gate is patterned on top of the heterostructure (Fig. 1, inset). Samples are cleaved in-situ, and the exposed (110) facet is overgrown

with a modulation-doping sequence. Applying a negative bias to the top gate depletes the 2DEG, leaving behind a 1D accumulation wire that is electrically contacted with the ungated 2DEG regions on either side.

Fig. 1, right displays the wire conductance G measured as a function of gate bias V_g at fixed temperature $T = 20$ and 340 mK , following illumination from the backside at $T \approx 10 \text{ K}$ with an infrared LED. The wire was biased with an excitation voltage $V_{ac} = 10 \text{ V} < 2k_B T/e$, where e is the electron charge. Each $G(V_g)$ trace corresponds to a different cooldown and illumination, and therefore to a slightly different electron density. Reproducible features appear in a 1:2:3 ratio along the G axis as steps close to $G = 0.44$ and $0.88e^2/h$, and as a change in average slope $dG(V_g) = dV_g$ at $G \approx 1.32e^2/h$, indicating a quantum conductance step $G_0 = 0.44e^2/h$. A conductance quantization of $0.44 \pm 0.05e^2/h$ was similarly observed in other samples. Below G_0 fluctuations are visible in the 340 mK trace, reminiscent of what is observed in disordered CEO GaAs wires [9, 10, 11]. Step-like features are observed below $T \approx 1 \text{ K}$.

More conductance steps appear with the application of a dc source-drain bias V (Fig. 1, left). The two lowest steps labeled 1 and 2 show stable step values comparable to those at $V = 0$, and other features labeled 3 and upwards show a step-like structure whose conductance values are increasingly dependent on the bias voltage. Comparing to the zero bias traces, one sees that the position of the first zero bias step has shifted from $V_g = 2.45 \text{ V}$ to 2.48 V . The clear step structure both at finite V and $V = 0$ is the strongest evidence of the 1D nature of our wires.

Strain is important in AlAs [12], so we pause to clarify its influence on the subband energies and valley degeneracy g_v in this structure before continuing with the analysis. In a local strain field, the strain components that control X -valley splitting are ϵ_{xx} , ϵ_{yy} and ϵ_{zz} for the X_x , X_y and X_z points, respectively. In 2D AlAs systems, strain splits the degeneracy of the valleys from a mean value E_0 by an amount ϵ [6], which is then compensated by the quantum confinement W in the z direction:

$$E_x = E_y = E_{xy} = E_0 + \frac{\hbar^2}{2m_L W^2} \quad (1)$$

$$E_z = E_0 + \frac{\hbar^2}{2m_H W^2} + \frac{\hbar^2}{2m_L W^2}$$

We simulated [13] these strain-induced splittings with matrix calculations of the 3-dimensional strain tensor [14] for 2D quantum well systems and verified the experimentally demonstrated degeneracy crossover $E_{xy} = E_z$ at $W = 60$ Å [6]. For the wider quantum wells of this work, the strain term dominates Eq. 1 and $E_{xy} < E_z$, yielding dual valley degeneracy.

For the CEO structure, we extended these strain calculations to determine the various spatially dependent X -band energies near the cleave plane. With $\hat{x}; \hat{y}; \hat{z} = [100]; [010]; [001]$ as unit vectors along the crystal axes, we define two other useful unit vectors $\hat{a} = (\hat{x} + \hat{y})/\sqrt{2} = [110]$ parallel to the wire, and $\hat{b} = (\hat{x} - \hat{y})/\sqrt{2} = [1\bar{1}0]$ normal to the cleave plane. The spatial dependence of strain in the $(\hat{b}; \hat{z})$ plane perpendicular to the wire is depicted in the color plot of Fig. 2 with red showing maximum compressive strain in the $\epsilon_{xx} = \epsilon_{yy}$ components in Fig. 2a, and red showing maximum tensile strain in ϵ_{zz} in Fig. 2b.

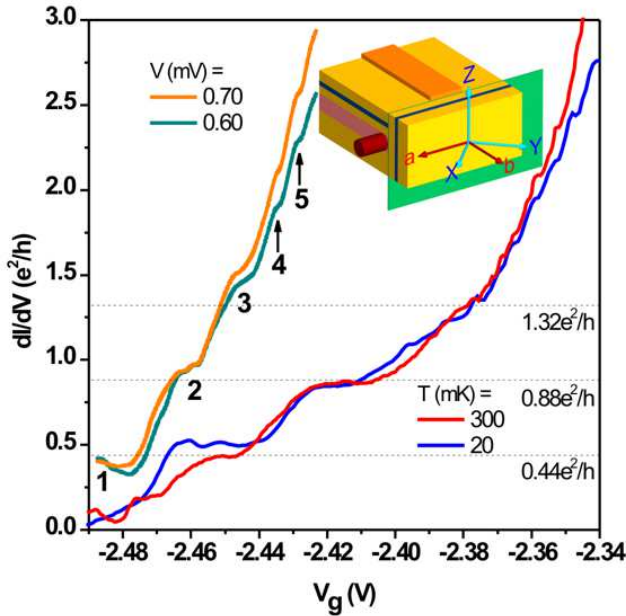


FIG. 1: (color online) Right: conductance G of an ÅÅ quantum wire as a function of gate bias V_g , at bath temperatures $T = 20$ mK (blue) and 300 mK (red) for two different cooldowns. Left: the population of higher 1D subbands (3, 4, 5) can be observed at $T = 20$ mK upon applying a finite source-drain dc bias V . Inset: schematic of the sample. The protruding red cylinder represents the wire at the edge of the ÅÅ 2DEG. Yellow: ÅÅ; blue: doping layers; green: cleave plane; orange: top gate.

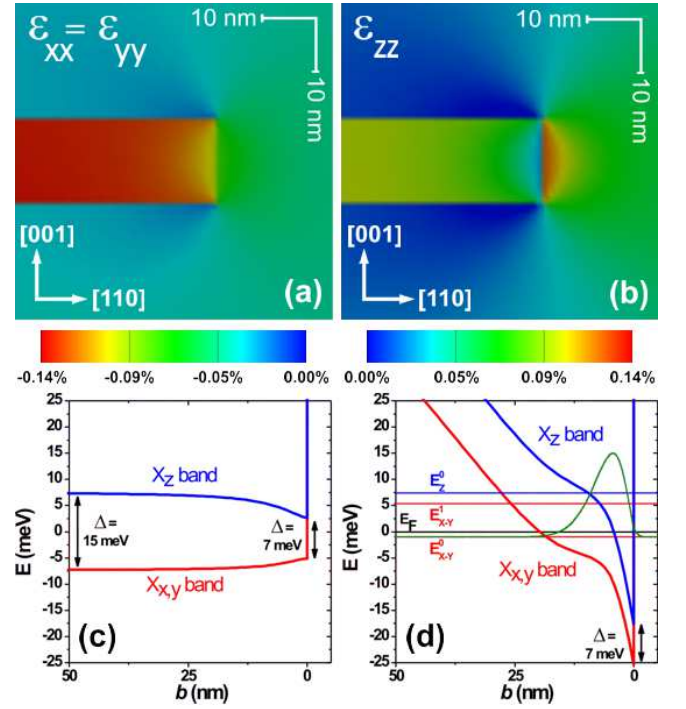


FIG. 2: (color online) Compressive (a) and tensile (b) strain components in the $(\hat{b}; \hat{z})$ plane. (c)–(d) X_{xy} and X_z band structure in the \hat{b} direction within the effective-mass approximation (distance is measured from the cleave plane). In (c) only strain is included. The energy E is offset by an arbitrary amount. In (d) both strain and electrostatics are computed. $E_i^{0,1}$ is the energy of the first, second X_{xy} 1D subband. $E_F = 0$ is the Fermi level. The probability density for the first X_{xy} 1D state is indicated.

The symmetry of the structure requires $\epsilon_{xx} = \epsilon_{yy}$, so the X_x and X_y valleys are shifted by the same amount and the valley degeneracy $g_v = 2$ in the lowest bands of the 2D well is preserved even in the wire region.

Fig. 2c shows the effect of strain alone (no doping) on the X_z and X_{xy} bands in the \hat{b} direction. Far from the cleave plane, the valley splitting of the band edges reaches 15 meV, however since both compressive $\epsilon_{xx} = \epsilon_{yy}$ and tensile ϵ_{zz} strain components decrease in magnitude at the cleave plane, the X_{xy} and X_z bands approach each other reaching a 7 meV separation at the cleave plane. In Fig. 2d the band calculation includes doping in the 2DEG and the overgrown structure; the 2DEG has been depleted underneath the gate. The energies of the first and second X_{xy} 1D subbands are still below the energy of the first X_z 1D subband.

Finally, we note the effect of the cleave-plane geometry on the 1D band mass. In units of the free electron mass, the scalar effective mass $m_{\hat{r}}$ projected along a given direction \hat{r} follows $1/m_{\hat{r}} = \sum_{jk} \hat{r}_j (\mathbf{m}^{-1})_{jk} \hat{r}_k$ with $(\mathbf{m}^{-1})_{jk}$ the inverse mass tensor, $m_{11} = m_H$; $m_{22} = m_{33} = m_L$; and $m_{jk} = 0$ for $j \neq k$. The result for unit vectors along

the wire \hat{a} and perpendicular \hat{b} are $m_a = m_b = 0.33 m_0$, almost a factor of 2 larger than m in (100) Si and a factor of 5 larger than m in GaAs wires. Using a calculated energy spacing between the first and second 1D subbands ~ 6 meV and a Fermi velocity v_F corresponding to the filling of the first subband, one sees that such a large m renders temperature irrelevant above 1 K as the thermal length $L_{th} = \hbar v_F / (2k_B T)$ exceeds the wire length $L = 1$ μ m.

We now discuss the experimentally measured step height $G_0 = 0.44e^2/h$, having clarified the effect of the strain and 1D confinement on the wire degeneracy. Within the Landauer-Buttiker formalism, the 1D conductance quantum reads $G_0 = g_s g_v e^2/h$, where $g_s = g_v = 2$ denotes the spin and valley degeneracy and τ is the transmission factor, so that $G_0 = 4e^2/h$ in the ballistic regime, almost a factor of 10 larger than measured.

Although a dominant factor in reducing GaAs CEO wire steps is 1D-2D non-adiabatic coupling, in these AlAs wires it cannot account for such a large reduction. Instead, the simplest explanation for the suppression of G_0 is a reduction of the transmission factor induced by the random distribution of backscattering centers. Those centers may be related to interface roughness or remote ionized dopants. Indeed, the absence of 'half plateaus' [15] in the differential conductance dI/dV as a function of V_g (see Fig. 1) may indicate that V drops at several scattering events along the wire. Disordered GaAs CEO wires of length $L > l_B^{wire}$, where l_B^{wire} is the backscattering length in the wire, also exhibit a largely reduced conductance: $G_0 \sim 0.4 - 2e^2/h$ [10, 11]. Following Ref. [16] we propose that under bias the transmission coefficient across the scattering potential landscape of the wire is averaged over a potential window of width eV, thereby averaging out conductance fluctuations and making higher 1D subband features apparent.

The assumption of a 4-fold degeneracy, however, is not straightforward in such 1D systems. The reduced conductance step might be partly due to a degeneracy lifting in the wire. For example, the so-called 0.7-structure was suggested to be a spontaneous spin-polarization at zero external magnetic field in GaAs QPC [17, 18]. In addition, $G_0 = 1e^2/h$ has recently been reported in single-walled carbon nanotubes [19], another two-band 1D material which in the absence of interactions should contain $g_v g_s = 4$ conductance modes. Such degeneracy-breaking in g_v or g_s are proposed to occur at sufficiently low densities above critical values of the Wigner-Seitz parameter r_s [20]. If we fill the first subband to 6 meV then the effective Bohr radius $a = 20$ \AA (using $m = 0.33 m_0$) yields $r_s = (2k_F g_v g_s a)^{-1} \sim 0.3$, where k_F denotes the Fermi wavevector in the wire, and $g_v = g_s = 2$. AlAs wires therefore reach an interesting regime for 1D systems, in that the second subband begins to become occupied while the first subband is still near the highly interacting $r_s \sim 1$ limit. Such strong interactions may

play a role in breaking the 4-fold spin/valley degeneracy, making this system of interest for future theoretical and experimental study.

In summary, we have measured conductance quantization in AlAs quantum wires with $G_0 \sim 0.44e^2/h$. Strain at the cleaved-edge should preserve the valley degeneracy $g_v = 2$ within the wire. G_0 is smaller than the single-channel conductance quantum, and is substantially reduced with respect to the conductance quantum $4e^2/h$ anticipated for spin- and valley-degenerate ballistic wires. This reduction suggests a backscattering-induced suppression of the transmission coefficient. A narrower gate and an enhanced 2DEG mobility may help access the ballistic regime in AlAs quantum wires.

J.M. and M.G. would like to thank C. Chamion, K. Kempa, and T. Giamarchi for helpful discussions. J.M. gratefully acknowledges support from the COLLECT-EC-Research Training Network, HPRN-CT-2002-00291.

Electronic address: moser@wisiu-muenchen.de

- [1] K. Nishiguchi and S. Oda, Appl. Phys. Lett. 76, 2922 (2000). K. Nishiguchi and S. Oda, J. Appl. Phys. 92, 1399 (2002).
- [2] S. L. Wang, P. C. van Son, B. J. Van Wees, and T. M. Klapwijk, Phys. Rev. B 46, 12873 (1992).
- [3] D. Tobben, D. A. Wharam, G. Abstreiter, J. P. Kotthaus, and F. Schäfer, Semicond. Sci. Technol. 10, 711 (1995); *ibid*, Phys. Rev. B 52, 4704 (1995).
- [4] U. Wieser, U. Kunze, K. Ismail, and J. O. Chu, Appl. Phys. Lett. 81, 1726 (2002).
- [5] S. Adachi, J. Appl. Phys. 58, R1 (1985).
- [6] H. W. van Kesteren, et al., Phys. Rev. B 39, 13426 (1989); A. F. W. van de Stadt, et al., Surface Science 361/362, 521 (1996).
- [7] A. Yacoby, et al., Solid State Comm. 101, 77 (1997).
- [8] E. P. De Poortere, Y. P. Shkolnikov, E. Tutuc, S. J. Padakis, and M. Shayegan, Appl. Phys. Lett. 80, 1583 (2002).
- [9] A. Yacoby, et al., Phys. Rev. Lett. 77, 4612 (1996).
- [10] O. M. Aulander, et al., Phys. Rev. Lett. 84, 1764 (2000).
- [11] M. Rother, Ph.D. Thesis (2000), Walter Schottky Institute, Techn. Univ. München (ISBN 3-932749-33-2).
- [12] Y. P. Shkolnikov, K. Vakil, E. P. De Poortere, and M. Shayegan, Phys. Rev. Lett. 92, 246804 (2004).
- [13] nextnano³ available at <http://www.nextnano.de>.
- [14] C. Herring, and E. Vogt, Phys. Rev. 101, 944 (1956).
- [15] L. P. Kouwenhoven, et al., Phys. Rev. B 39, 8040 (1989).
- [16] P. F. Bagwell and T. P. Orlando, Phys. Rev. B 40, 1456 (1989).
- [17] K. J. Thomas, J. T. Nicholls, M. Y. Simmons, M. Pepper, D. R. Mace, and D. A. Ritchie, Phys. Rev. Lett. 77, 135 (1996).
- [18] A. C. G. Raham, et al., Phys. Rev. Lett. 91, 136404 (1993).
- [19] M. J. Biercuk, N. Mason, J. Martin, A. Yacoby, and C. M. Marcus, Phys. Rev. Lett. 94, 026801 (2005).
- [20] L. Calmels and A. Gold, Europhys. Lett. 39(5), 539 (1997).